Influence of Dangling Thymidine Residues on the Stability and Structure of Two DNA Duplexes†

Mary Senior, Roger A. Jones, and Kenneth J. Breslauer*
Department of Chemistry, Rutgers, The State University of New Jersey, New Brunswick, New Jersey 08903
Received October 23, 1987; Revised Manuscript Received January 19, 1988

ABSTRACT: We have employed temperature-dependent UV spectroscopy, circular dichroism (CD), 400-MHz proton nuclear magnetic resonance (NMR), and computer modeling to characterize both structurally and thermodynamically the influence of unpaired, dangling thymidine residues (T) on the thermal stability and melting behavior of two DNA core duplexes. The specific DNA double helices that we have investigated in this work are core duplexes $\{d(GC)_3\}_2$ (I) and $\{d(CG)_3\}_2$ (IV), 3′ dangling T derivatives $\{d[(GC)_3TT]\}_2$ (II) and $\{d[(CG)_3TT]\}_2$ (V), and 5′ dangling T derivatives $\{d[TT(GC)_3]\}_2$ (III) and $\{d[TT(CG)_3]\}_2$ (VI). Our experimental data allow us to reach the following conclusions: (1) For both core duplexes (I and IV), the addition of dangling T residues on either the 5′ or 3′ end causes an increase in the optical melting temperature t_m. (2) For both core duplexes, 5′ dangling T residues induce a greater increase in the optical t_m's than 3′ dangling T residues. (3) For both cores duplexes, the increase in t_m induced by the addition of dangling T residues is enthalpic in origin, with 5′ dangling T residues inducing a greater increase in the van't Hoff transition enthalpy than 3′ dangling T's. (4) Dangling T residues cause downfield shifts in all of the nonexchangeable aromatic protons of the $\{d(GC)_3\}_2$ core duplex (I), with the 5′ T residues inducing the largest shifts. For the most part, this trend does not hold with the $\{d(CG)_3\}_2$ core duplex (IV). (5) For both core duplexes, the addition of dangling T residues causes an increase in the NMR t_m's of almost all the nonexchangeable aromatic protons of the core duplex. This increase generally is greater when the dangling T residues are attached to the 5′ end of the core duplex. (6) For both core duplexes, the unpaired T residues exhibit NMR melting temperatures that are close to the global optical t_m's of the duplex structures. (7) At low temperatures, the dangling T residues exhibit chemical shifts that are consistent with their stacking on the core duplex. (8) CD spectra of both core duplexes and their corresponding dangling T derivatives are consistent with all six structures existing in the B conformation. These experimental results, in conjunction with computer modeling, support a picture in which the dangling T residues increase the thermal stability of their core duplexes by causing an increase in enthalpically favorable interactions. We propose that these enthalpically favorable interactions result from two effects: (i) stacking of the dangling T residues on the base-paired termini of the core duplex and (ii) an increase in stacking within the core duplex induced by the presence of the dangling ends. Significantly, the increase in thermal stability and transition enthalpy induced by the dangling thymidine residues is greatest when the unpaired residues are positioned on the 5′ end of the core duplexes. The Turner group has shown that dangling ends on RNA core duplexes exhibit the opposite positional dependence [Petersheim, M., & Turner, D. H. (1983) *Biochemistry 22*, 256–263; Freier, S. M., Alkema, D., Sinclair, A., Neilson, T., & Turner, D. H. (1985) *Biochemistry 24*, 4533–4539], with 3′ rather than 5′ dangling residues exerting the greatest influence.

Terminal, unpaired bases adjacent to stretches of duplex regions are found in many RNA molecules involved in biological processes. Such "dangling ends" have been shown to increase the thermal stability of RNA duplexes (Martin et al., 1971; Romaniuk et al., 1978; Petersheim & Turner, 1983; Freier et al., 1985, 1986a; Sugimoto et al., 1987). As noted by the Turner group (Sugimoto et al., 1987), this influence of dangling ends may be important in modulating biological processes such as codon–anticodon associations (Grosjean et al., 1976; Yoon et al., 1976), tertiary structure formation in tRNA (Kim et al., 1974; Robertus et al., 1974), and codon context effects (Ayer & Yarus, 1986). In addition, the Turner group has demonstrated that biophysical studies on RNA duplexes with dangling ends provide a unique opportunity to resolve base stacking and base pairing contributions to RNA duplex stability (Turner et al., 1987).

Dangling ends also may play an important role in modulating biological processes involving DNA duplexes. Nevertheless, the literature is nearly void of parallel DNA studies on deoxyoligonucleotides with and without dangling ends. The one exception is a study in which the self-complementary sequence d(TCG) was found to form a miniduplex at 5 °C, while the self-complementary sequence d(CGT) did not form a miniduplex (Mellema et al., 1984). However, interpretation and quantification of the data from this study were difficult due to the low melting temperatures of such short duplexes and because of the absence of a comparative study on the corresponding core duplex $\{d(CG)\}_2$. To alleviate this situation, we have begun a program to synthesize and to study stable deoxy core duplexes with dangling residues on either the 3′ or 5′ end.

In this work, we have studied the influence of dangling thymidine residues on two self-complementary hexameric core molecules. The specific structures we have investigated are

$\{d(CG)_3\}_2$	$\{d[TT(CG)_3]\}_2$	$\{d[(CG)_3TT]\}_2$
I	II	III
$\{d(GC)_3\}_2$	$\{d[TT(GC)_3]\}_2$	$\{d[(GC)_3TT]\}_2$
IV	V	VI

†This work was supported by NIH Grants GM23509 (K.J.B.) and GM31483 (R.A.J.).
*Author to whom correspondence should be addressed.

0006-2960/88/0427-3879$01.50/0

The core or parent duplex molecules, I and IV, were chosen because they form stable helices well above 0 °C and because they melt in a cooperative manner, thereby simplifying the thermodynamic analysis (Senior et al., 1985; Albergo et al., 1981; Marky et al., 1985; Breslauer et al., 1986; Breslauer, 1986). The four dangling thymidine (T) derivatives of these two core duplexes (II, III, V, and VI) were designed to allow us to define the influence of 5′ versus 3′ dangling thymidine residues on the structures and melting behaviors of the associated duplexes. In this paper, we report and compare the results of our structural and thermodynamic characterizations of these six duplex structures.

Experimental Procedures

Materials

Deoxynucleotide Synthesis. Molecules I–VI were synthesized by a solid-phase phosphoramidite procedure (Gaffney et al., 1984) either manually or on a Biosearch 8600 synthesizer. Deprotection and high-performance liquid chromatography (HPLC) purification were carried out as reported previously (Gaffney et al., 1984). For characterization, each pure deoxy oligomer was degraded to its constitutent deoxynucleosides by using a mixture of venom phosphodiesterase and alkaline phosphatase (Sigma Chemical Co., St. Louis, MO). For each sequence, the expected ratio of monomers was found. The HPLC chromatograms of each pure sequence and of the mixture of deoxynucleosides obtained upon enzymatic degradation are available (see paragraph at end of paper regarding supplementary material).

Solution Preparation. Oligomer solutions were prepared using a buffer system containing 10 mM sodium phosphate and 0.1 mM ethylenediaminetetraacetic acid (EDTA), with the final pH adjusted to 7.0. Sodium chloride was added to bring the final concentration to 1.0 M. For each solution, the concentration of the oligomer in single strands was spectroscopically determined. To accomplish this, the 25 °C extinction coefficients (ϵ) were calculated for each sequence using a nearest-neighbor analysis (Cantor et al., 1970; Richards, 1975). We obtained the following ϵ ($\times 10^4$ M^{-1} cm^{-1}) values at 280 nm: $\{d(GC)_3\}_2$, 4.85; $\{d[TT(GC)_3]\}_2$, 5.55; $\{d[(GC)_3TT]\}_2$, 4.89; $\{d(CG)_3\}_2$, 4.00; $\{d[TT(CG)_3]\}_2$, 5.10; $\{d[(CG)_3TT]\}_2$, 5.27. These ϵ values then were used to calculate the concentration of each solution by application of Beer's law. For this calculation, the slope of the upper baseline in each UV melting curve was extrapolated to low temperature to determine the single strand absorbance at 25 °C. The range of concentrations used in the optical studies was from 10^{-6} to 10^{-4} M in single strands.

NMR Deoxynucleotide Solutions. Each oligomer solution was prepared for NMR studies by first converting to the sodium salt. This conversion was accomplished by ion-exchange chromatography using a short (1 × 10 cm) column of sodium form ion-exchange resin. The oligomer then was eluted with water. The appropriate fractions were lyophilized and redissolved in a buffer containing 0.010 M phosphate, 0.01 M EDTA, and 1.0 M NaCl, with the final pH adjusted to 7.0. The resulting solution was lyophilized and then dissolved in 99.8 atom % D D_2O (Aldrich). For each oligomer, this procedure was repeated, and each final sample was dissolved in 0.5 mL of 100 atom % D D_2O (Aldrich). The following concentrations (in mmol/L) of single strands were used to measure chemical shift versus temperature profiles: $\{d(GC)_3\}_2$, 0.95; $\{d[TT(GC)_3]\}_2$, 0.83; $\{d[(GC)_3TT]\}_2$, 0.94; $\{d(CG)_3\}_2$, 1.15; $\{d[TT(CG)_3]\}_2$, 0.90; $\{d[(CG)_3TT]\}_2$, 0.88. Chemical shifts of the nonexchangeable protons were obtained by indirect reference to the sodium salt of the standard (trimethylsilyl)-propanesulfonic acid (TSP). This method makes the reasonable assumption that HDO and H_2O have identical chemical shifts relative to TSP in the buffer system used in these experiments.

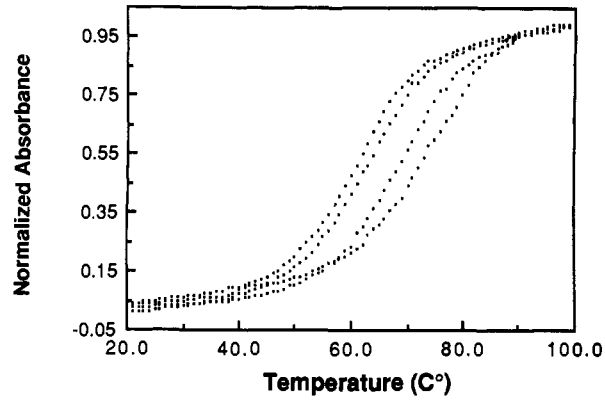

FIGURE 1: Normalized absorbance versus temperature profiles at different strand concentrations for $\{d[TT(GC)_3]\}_2$ in 1 M NaCl and 10 mM phosphate buffer, pH 7.0.

Deoxyoligonucleotide solutions for nuclear Overhauser effect (NOE) experiments were prepared in the same manner except that the final sodium cation concentration for molecules I, IV, and VI was 0.1 M. This lower salt buffer is used to avoid aggregation at the higher NMR concentrations. For this buffer system, the following 95 °C extinction coefficients at 280 nm in units of 10^4 M^{-1} cm^{-1} were used to calculate the concentrations of the three duplexes: $\{d(GC)_3\}_2$, 4.79; $\{d[TT(CG)_3]\}_2$, 5.51; $\{d[(CG)_3TT]\}_2$, 4.96. The following concentrations (in mmol/L) of single strands were used in the NOE experiments: $\{d(GC)_3\}_2$, 3.76; $\{d[TT(GC)_3]\}_2$, 1.70; $\{d[(GC)_3TT]\}_2$, 1.11; $\{d[TT(CG)_3]\}_2$, 2.00; $\{d[(CG)_3TT]\}_2$, 5.59.

Methods

UV Absorbance Spectroscopy. Absorbance versus temperature profiles were obtained at 280 nm on a Perkin-Elmer 575 spectrophotometer. Data acquisition and analysis were performed on a Tektronix 4051 computer interfaced to the spectrophotometer. Optical cells were used with pathlengths of 0.1, 0.2, 0.5, and 1.0 cm, thereby facilitating measurements over a range of oligomer concentrations. The temperature in each run was increased continuously from 20 to 100 °C at a rate of 0.5 °C/min. A total of 400 data points were collected for each melting curve.

Thermodynamic Analysis of Optical Melting Data. To extract thermodynamic data from absorbance versus temperature profiles, we determined UV melting curves over a range of strand concentrations. Figure 1 shows a typical family of concentration-dependent melting curves we have measured for one of our six duplex structures. The t_m data from such a family of curves allow us to construct a $1/T_m$ versus ln C_T plot, where C_T equals the total concentration in single strands and $1/T_m$ is the reciprocal of the melting temperature in Kelvin. Figure 2 shows the $1/T_m$ versus ln C_T plots we have determined for all six duplex structures investigated in this work. As previously described (Martin et al., 1971; Breslauer et al., 1975; Albergo et al., 1981; Marky & Breslauer, 1987), such plots can be analyzed by using the following equation to derive van't Hoff enthalpy and entropy data.

$$\frac{1}{T_m} = \frac{R}{\Delta H_{VH}} \ln C_T + \frac{\Delta S}{\Delta H_{VH}} \quad (1)$$

The van't Hoff transition enthalpy can be calculated from the

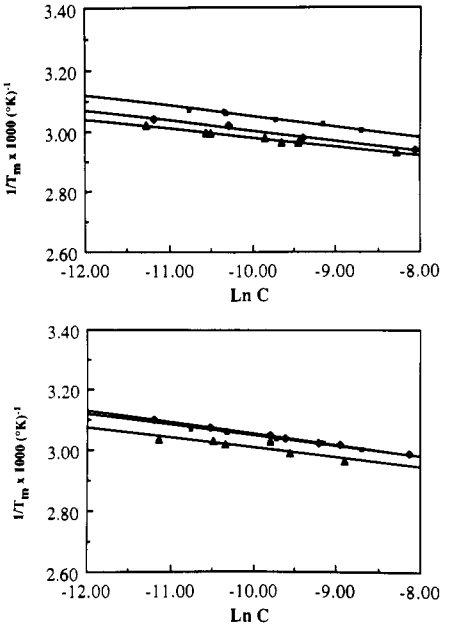

FIGURE 2: (Upper panel) Plots of $1/T_m$ versus ln C for the $\{d(GC)_3\}_2$ family: (■) $\{d(GC)_3\}_2$; (♦) $\{d[(GC)_3TT]\}_2$; (▲) $\{d[TT(GC)_3]\}_2$. (Lower panel) Plots of $1/T_m$ versus ln C for the $\{d(CG)_3\}_2$ family: (■) $\{d(CG)_3\}_2$; (♦) $\{d[(CG)_3TT]\}_2$; (▲) $\{d[TT(GCGC)_3]\}_2$. All experiments in 1 M NaCl and 10 mM phosphate buffer, pH 7.0.

slope of the $1/T_m$ versus ln C_T plot while the entropy can be determined from the intercept. This analysis of the optical melting data assumes a two-state transition for the helix-to-coil transition (Breslauer, 1986).

Circular Dichroism (CD) Spectroscopy. Circular dichroism spectra were recorded on a Model 60DS Aviv spectropolarimeter equipped with a programmable, thermoelectrically controlled cell holder. The spectropolarimeter is interfaced to a computer for data acquisition and processing (Aviv Associates, Lakewood, NJ). Each spectrum shown here corresponds to an average of at least three scans.

NMR Techniques. NMR experiments were performed on a Varian XL-400 MHz spectrometer with a 32-bit microprocessor for data acquisition and analysis. The temperature of the sample was maintained by a Varian temperature-control unit. This unit was calibrated using neat ethylene glycol. This calibration allowed us to correct the digital output of the unit so as to reflect the true temperature of the sample. For the measurements reported here, this correction never exceeded 1.2 °C. Chemical shift versus temperature plots were determined by changing the temperature in 5–10 °C increments over the range of 0–95 °C. The samples were allowed to equilibrate for a minimum of 15 min at each temperature before acquisition was initiated. Several hundred free induction decays (FID's) were required for each sample at a given temperature. Resonance assignments for the duplex nonexchangeable protons for molecules I–III are those of Cheng et al. (1984). It is assumed that the assignments of the aromatic nonexchangeable core protons in our duplexes are not affected by the presence of the unpaired T's. Resonance assignments for the nonexchangeable aromatic base protons for molecules IV–VI were made by utilizing the nuclear Overhauser effect (NOE) as previously described by Petersheim and Turner (1983). NOE's were obtained for $\{d(GC)_3\}_2$ at 10.5 °C by selectively irradiating the aromatic and the sugar H1′ protons for 0.3 s prior to acquisition. Spectra were accumulated simultaneously by array cycling to minimize systematic changes in the sample and the spectrometer. Fourier transforms were obtained in the double-precision mode to improve accuracy. NOE's between the sugar and the aromatic base protons were observed with NOE difference spectra. Assignments of the thymidine base protons were made for molecules II, III, V, and VI by selectively irradiating the TH6 and methyl protons in each duplex.

Table I: Optical Melting Temperatures, t_m, in 1 M NaCl and at a Strand Concentration of 10^{-5} M[a]

duplex no.	structure	t_m (°C)	Δt_m (°C)
I	$\{d(GC)_3\}_2$	49.2	
II	$\{d[(GC)_3TT]\}_2$	54.2	5.0
III	$\{d[TT(GC)_3]\}_2$	57.5	8.3
IV	$\{d(CG)_3\}_2$	45.3	
V	$\{d[(CG)_3TT]\}_2$	48.3	3.0
VI	$\{d[TT(CG)_3]\}_2$	54.4	9.1

[a] We estimate the uncertainty in the t_m data to be ±0.5 °C.

Results and Discussion

Influence of Dangling Thymidine Residues on Duplex Melting Temperatures. We have measured absorbance versus temperature profiles for the "melting" or our two parent core duplexes $\{d(GC)_3\}_2$ and $\{d(CG)_3\}_2$ and their associated 5′ and 3′ dangling thymidine derivatives (structures II, III, V, and VI). Representative concentration-dependent melting curves are shown in Figure 1 for $\{d[TT(GC)_3]\}_2$. We analyzed these optical melting curves using previously described methods to obtain melting temperatures, t_m's, for each transition (Breslauer, 1986; Marky & Breslauer, 1987). The resulting t_m values for the two core duplexes and their corresponding dangling T derivatives are listed in Table I. These tabulated melting temperatures are concentration dependent since duplex formation is bimolecular. Consequently, to allow for meaningful comparisons between different duplex structures, all the t_m values listed in Table I correspond to a common concentration of 10^{-5} M in single strands. In the final column of Table I, we also list Δt_m values. This parameter corresponds to the difference in melting temperatures between each core duplex and its corresponding dangling thymidine derivatives at 10^{-5} M in single strands.

Inspection of the t_m and Δt_m data listed in Table I allows us to reach the following conclusions:

(1) The $\{d(GC)_3\}_2$ core duplex is thermally more stable than the $\{d(CG)_3\}_2$ core duplex. This sequence-dependent differential thermal stability is consistent with previous reports for both RNA duplexes (Freier et al., 1985) and DNA duplexes (Marky & Breslauer, 1984; Breslauer et al., 1986).

(2) Both 5′ and 3′ dangling thymidine residues increase the thermal stabilities (t_m's) of their duplex structures relative to their corresponding parent core duplexes.

(3) 5′ dangling thymidine residues induce a greater increase in t_m than do 3′ dangling thymidine residues. This result holds for both core duplexes. Significantly, this positional dependence for the thermal stability induced by dangling thymidine residues in DNA duplexes is just the opposite of that reported for RNA duplexes (Petersheim & Turner, 1983; Freier et al., 1986). Later in this paper, we propose a possible structural interpretation for this contrasting influence of dangling ends on the thermal stabilities of RNA and DNA duplexes.

We consider the conclusions listed above to be well founded since they are based on t_m measurements that are accurate to better than ±0.5 °C, and which are not particularly sensitive to the assumed two-state nature of the transition. In the sections that follow, we present additional data which allow us to characterize the *thermodynamic origins* of the dangling thymidine induced changes in melting temperatures listed in

Table II: Enthalpy and Entropy Data Derived from the Concentration Dependence of Optical Melting Temperatures[a,b]

duplex no.	structure	$\Delta H°$	$\Delta\Delta H°$	$\Delta S°$	$\Delta\Delta S°$
I[c]	$\{d(GC)_3\}_2$	59.1		160.4	
II	$\{d[(GC)_3TT]\}_2$	60.0	0.9	160.4	0.0
III	$\{d[TT(GC)_3]\}_2$	67.0	7.9	179.9	9.5
IV	$\{d(CG)_3\}_2$	46.4		122.8	
V	$\{d[(CG)_3TT]\}_2$	54.8	8.4	147.6	24.8
VI	$\{d[TT(CG)_3]\}_2$	62.2	15.8	167.2	44.4

[a] Enthalpies in kcal/mol and entropies in cal/(mol·K) are derived from the respective slopes and intercepts using eq 1. $\Delta\Delta H$ and $\Delta\Delta S$ values correspond to the differences in enthalpy and entropy changes between the dangling thymidine derivatives and their corresponding parent core duplexes. [b] Estimated errors in $\Delta H°$ and $\Delta S°$ are ±5%. [c] The $\Delta H°$ and $\Delta S°$ values determined in this work for the $\{d(GC)_3\}_2$ duplex are in excellent agreement with a previously reported study on the same duplex (Albergo et al., 1981).

Table III: Comparison of Free Energy of Stabilization Induced by a Dangling Thymidine Residue and by an Additional AT Base Pair[a]

duplex no.	structure	$\Delta G°_{25}$	$-\Delta\Delta G°/2$	$-\Delta\Delta G°_{bp}$[b]
I	$\{d(GC)_3\}_2$	11.3		
II	$\{d[(GC)_3TT]\}_2$	12.2	0.4	1.6
III	$\{d[TT(GC)_3]\}_2$	13.4	1.0_5	1.9
IV	$\{d(CG)_3\}_2$	9.8		
V	$\{d[(CG)_3TT]\}_2$	10.8	0.5_0	1.3
VI	$\{d[TT(CG)_3]\}_2$	12.4	1.3_0	1.6

[a] Free energies are in kcal/mol. [b] From Breslauer et al. (1986).

Table I. The "conclusions" that we will derive from the thermodynamic data are more qualitative than those based exclusively on t_m and Δt_m data since transition enthalpies and entropies cannot be determined as accurately as melting temperatures. This lower accuracy is exacerbated by the fact that we will be comparing small differences between large numbers. Nevertheless, if one keeps these limitations in mind, it still is useful to examine the thermodynamic origins of the melting temperature trends noted above and reflected in the data listed in Table I.

Thermodynamic Consequences of Dangling Thymidine Residues. Figure 2 shows the $1/T_m$ versus ln C_T plots we have determined for all six duplex structures investigated in this work. From the slopes and the intercepts of these lines, we have calculated the enthalpy and entropy data listed in Table II. Inspection of these thermodynamic data reveals the following observations:

(1) The lower t_m of the $\{d(CG)_3\}_2$ core duplex compared with that of the $\{d(GC)_3\}_2$ core duplex is due to a reduced transition enthalpy.

(2) The increase in t_m induced by both 5′ and 3′ dangling thymidine residues is enthalpic in origin for all four duplex structures investigated in this work. This observation is consistent with the results of the Turner group on the thermodynamic origin of dangling end induced stabilization for RNA duplexes (Freier et al., 1986c; Turner et al., 1987).

(3) 5′ dangling T residues increase t_m values more than 3′ dangling T residues because they induce a greater increase in the transition enthalpies of their duplexes. In other words, for both core duplexes, 5′ dangling T residues (duplexes III and VI) are enthalpically more favorable than 3′ dangling T residues (duplexes II and V).

To evaluate the influence, if any, of the base-paired residue directly adjacent to the dangling thymidines, we also have calculated the $\Delta\Delta H°$ and the $\Delta\Delta S°$ data listed in Table II. These data were derived by taking the differences between the enthalpy and entropy changes for each dangling end duplex and its corresponding core duplex. Inspection of these data suggests that the exact magnitude of $\Delta H°$ or $\Delta S°$ for each dangling end duplex depends on the nature of the base-paired residue adjacent to the unpaired thymidines. For example, it appears that more favorable enthalpic interactions result when 3′ dangling thymidines are on the same strand and adjacent to a G residue (duplex, V, $\Delta\Delta H°$ = 8.4 kcal/mol) rather than a C residue (duplex II, $\Delta\Delta H°$ = 0.9 kcal/mol). The opposite neighboring residue effect appears to hold for 5′ dangling thymines (duplex III, $\Delta\Delta H°$ = 7.9 kcal/mol, versus duplex VI, $\Delta\Delta H°$ = 15.8 kcal/mol). Although these more quantitative conclusions are consistent with the data listed in Table II, they should be viewed with extreme caution since the $\Delta\Delta H°$ differences on which they are based fall within the error limits of the thermodynamic data.

In an effort to more directly and more accurately measure the transition enthapies of each duplex structure, we also have employed differential scanning calorimetry (DSC) (Senior and Breslauer, unpublished results). However, these measurements were conducted at significantly higher strand concentrations where the duplexes with dangling thymidine residues appear to exhibit intermolecular effects (e.g., aggregation) that we do not observe at the lower optical and NMR concentrations used in this work. Consequently, the results of our DSC studies cannot be reported until we have characterized the influence of these concentration-induced intermolecular effects on our calorimetric data. In this paper, we will rely on the two-state thermodynamic data presented above which were derived from optical melting studies using the protocols described under Methods.

Influence of a Dangling Thymidine Residue versus an Additional AT Base Pair. For each core duplex, it is of interest to compare the stabilization induced by a dangling T residue with the stabilization that would result if the core duplex was extended by one AT base pair. To make this comparison, we have calculated the free energy data compiled in Table III. The first data column lists the free energy change for the disruption of each duplex structure at 25 °C. These $\Delta G°_{25}$ values were calculated from the $\Delta H°$ and $\Delta S°$ data listed in Table II using the standard thermodynamic relationship $\Delta G° = \Delta H° - T\Delta S°$. The second data column of Table III lists the differences in $\Delta G°_{25}$ values per thymidine residue between each dangling end duplex and its corresponding core duplex (I or IV). These $\Delta\Delta G°$ data are divided by 2 so as to reflect the influence of a single dangling thymidine residue. The resulting $\Delta\Delta G°/2$ values provide a measure of the stabilizing influence that a single dangling T residue imparts to its core duplex. Inspection of these $\Delta\Delta G°/2$ values reveals that for both core duplexes (I and IV) a 5′ dangling T residue is more stabilizing than a 3′ dangling T residue. [Recall that we reached a similar conclusion exclusively on the basis of t_m and Δt_m data (see Table I).] Significantly, this positional dependence is just the opposite of that reported by the Turner group for the influence of dangling residues on RNA duplexes (Freier et al., 1985).

The last column in Table III lists the free energy increment that would result from extending each core duplex by a single AT base pair at either its 5′ or its 3′ end ($\Delta\Delta G°_{bp}$). These values were obtained from the published thermodynamic library of DNA nearest-neighbor interactions (Breslauer et al., 1986). By comparing the data in the last two columns of Table III, we obtain a comparison between the stabilizing influence of a dangling T residue ($\Delta\Delta G°/2$) and the stabilizing influence of an additional AT base pair ($\Delta\Delta G°_{bp}$). Inspection of these data reveals that a dangling T residue can impart between 30% and 80% of the stabilization induced by an additional AT base pair. The exact magnitude of this effect depends on the

Table IV: Proton Chemical Shifts (ppm) for the Nonexchangeable Base Protons of the $\{d(GC)_3\}_2$ and $\{d(CG)_3\}_2$ Families in 1 M NaCl[a]

proton	$\{d(GC)_3\}_2$	$\{d[(GC)_3TT]\}_2$	$\{d[TT(GC)_3]\}_2$
	(a) $\{d(GC)_3\}_2$ Family		
TH6			7.76
$T(CH_3)$			2.05
TH6			7.73
$T(CH_3)$			1.97
GH8	8.35	8.36	8.36
CH5	5.44	5.78	*b*
CH6	7.38	7.71	7.66
GH8	7.86	8.21	8.24
CH5	5.53	5.78	*b*
CH6	7.33	7.63	7.71
GH8	7.90	8.21	8.24
CH5	5.27	5.30	*b*
CH6	7.44	7.71	7.81
TH6		7.83	
$T(CH_3)$		1.88	
TH6		7.94	
$T(CH_3)$		2.13	
	(b) $\{d(CG)_3\}_2$ Family		
proton	$\{d(CG)_3\}_2$	$\{d[(CG)_3TT]\}_2$	$\{d[TT(CG)_3]\}_2$
TH6			7.80
$T(CH_3)$			1.94
TH6			7.78
$T(CH_3)$			1.86
CH5	6.11	6.12	5.93
CH6	7.79	7.67	7.89
GH8	8.12	8.18	8.17
CH5	5.76	5.64	5.70
CH6	7.54	7.43	7.61
GH8	8.08	8.07	8.14
CH5	5.86	5.64	5.79
CH6	7.54	7.36	7.58
GH8	8.08	8.09	8.17
TH6		7.53	
$T(CH_3)$		1.75	
TH6		7.56	
$T(CH_3)$		1.73	

[a] Chemical shifts are referenced to the standard TSP. [b] Proton was not assigned due to spectral overlap.

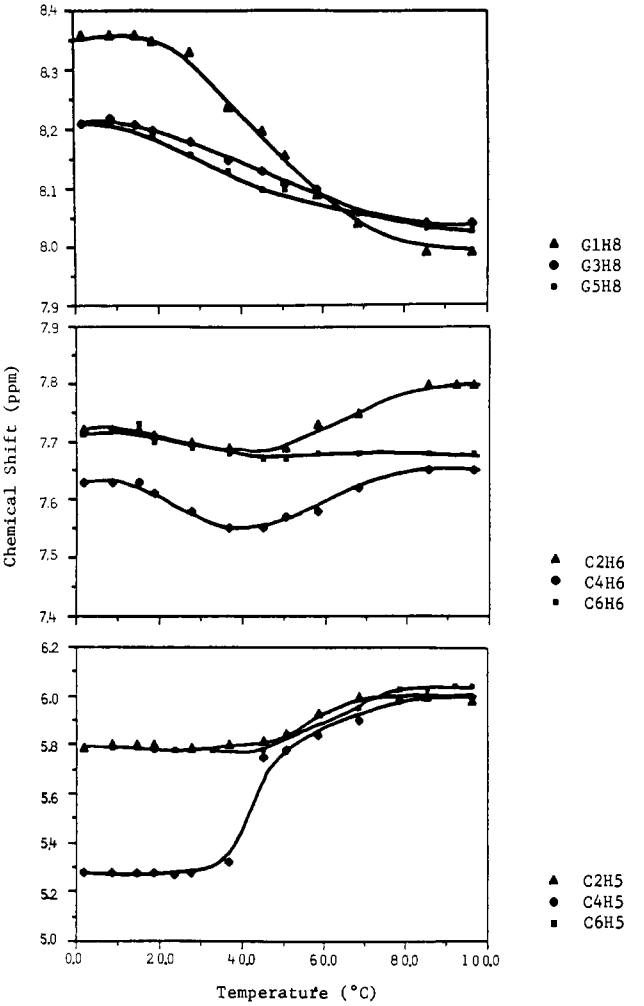

FIGURE 3: Temperature dependence of the base proton resonances of $\{d(GCGCGCTT)\}_2$ in 1 M NaCl and 10 mM phosphate buffer. Chemical shifts were referenced externally to the TSP standard.

position of the dangling end (5′ versus 3′) and the nature of the core duplex (or the terminal base pair) on which the dangling residue is stacked. Thus, for the DNA duplexes investigated here, a dangling T residue can impart a significant fraction of the stabilization that would result if either core duplex was extended by an additional AT base pair.

CD Spectroscopy. We employed CD spectroscopy to characterize the global conformations of our two core duplexes and their associated dangling thymidine derivatives. The CD spectra we obtained are available as supplementary material. Significantly, each spectra exhibits a CD profile that qualitatively is consistent with a duplex in the B conformation. Thus, for the sequences studied in this work, addition of the dangling thymidine residues does not alter the global conformation of the core duplexes as monitored by CD spectroscopy. To provide a more microscopic view of the consequences of the dangling T residues, we have employed proton NMR as described below.

NMR Studies. As noted under Methods, we have used 400-MHz NMR to assign resonances and to monitor the thermally induced helix-to-coil transitions of the two core duplexes and their corresponding dangling thymidine derivatives. In the sections that follow, we present our NMR results and explain how they provide us with a microscopic framework within which to interpret some of our thermodynamic data.

Chemical Shift Data. Table IV lists the proton chemical shifts of the nonexchangeable aromatic base protons associated with each duplex structure at 10 °C, a temperature at which the duplexes are fully formed. Inspection of the data in Table IVa reveals that the addition of either 5′ or 3′ dangling thymidine residues to the $\{d(GC)_3\}_2$ duplex causes the nonexchangeable aromatic base protons of the core residues to shift downfield relative to their positions in the parent duplex. For all but one proton, this shift is greater when the dangling thymidines are on the 5′ end of the $\{d(GC)_3\}_2$ duplex. Inspection of the data in Table IVb reveals that this trend is not as evident in the $\{d(CG)_3\}_2$ family, although dangling thymidines on the 5′ end of the core duplex once again cause more downfield shifts in the nonexchangeable aromatic base protons of the core duplex than dangling thymidines on the 3′ end. Taken together, the chemical shift data listed in Table IV suggest that the unpaired T residues exhibit an influence on the conformations of the core duplex regions.

Chemical Shift versus Temperature Data. We also have used NMR to monitor the thermally induced helix-to-coil transitions of each core duplex and their associated dangling thymidine derivatives. Typical chemical shift versus temperature plots are shown in Figures 3 and 4. In Figure 3, we monitored the nonexchangeable aromatic base protons while in parts a and b of Figure 4 we monitored the CH_3 and the TH6 protons, respectively of the dangling thymidine residues. Assuming on the NMR time scale that these helices are in fast exchange with their single strands, we obtained NMR melting temperatures by analyzing the shapes of those chemical shift versus temperature curves that exhibited clear transition regions and well-defined baselines. The resulting

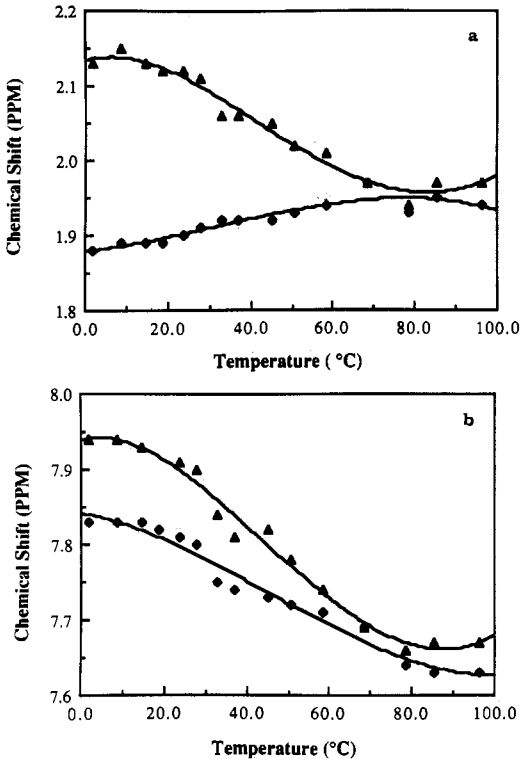

FIGURE 4: (Panel a) Temperature-dependent chemical shifts of the dangling methyl resonances [(♦) CH_3(A); (▲) CH_3(B)] of {d-(GCGCGCTT)}$_2$ in 1 M NaCl and 10 mM phosphate buffer, pH 7.0. Chemical shifts were referenced externally to the TSP standard. (Panel b) Temperature-dependent chemical shifts of the dangling TH6 resonances [(♦) TH_6(A); (▲) TH_6(B)] of {d(GCGCGCTT)}$_2$ in 1 M NaCl and 10 mM phosphate buffer, pH 7.0. Chemical shifts were referenced externally to the TSP standard.

t_m data are tabulated in Table V. Footnote *a* in Table V indicates that the shape of the chemical shift versus temperature profile did not permit a melting temperature to be defined. Inspection of the data in Table V reveals that addition of dangling thymidine residues induces an increase in the NMR t_m's of the nonexchangeable aromatic protons associated with most of the core bases. It should be noted that, with a few exceptions, the 5′ dangling thymines induce a greater increase in the NMR t_m's of the core protons than the 3′ dangling thymidine residues. A crude comparison can be made between these local NMR t_m values and our global optical melting data by defining an "average NMR t_m" value (see data at the bottom of each column in parts a and b of Table V). We calculated this global NMR melting temperature as the average of the local t_m values of each core proton (the t_m's of the dangling thymidine are not included). Significantly, these microscopic NMR t_m values reveal the same qualitative trend as that exhibited by the optical t_m data; namely, the addition of dangling thymidine residues causes an increase in the melting temperature of the overall structure, with 5′ dangling T residues being more effective than 3′ dangling T residues. Thus, the NMR and the optical results provide a consistent picture.

"Melting" of the Dangling Thymidine Residues. Inspection of the t_m data in Table V reveals that with one exception the dangling thymidine residues exhibit relatively high melting temperatures. This observation is particularly true of the 5′ thymidine residue directly adjacent to the core duplex and to a lesser extent for both 3′ dangling thymidine residues. Thus, both the chemical shift and NMR t_m data suggest a picture in which the 5′ and 3′ dangling thymidine residues are stacked on the core duplex.

Table V: NMR Melting Temperatures (°C), t_m, for the Nonexchangeable Base Protons of the {d(GC)$_3$}$_2$ and {d(CG)$_3$}$_2$ Families

proton	{d(GC$_2$GC$_4$GC$_6$)}$_2$	{d[(GC)$_3$T$_A$T$_B$]}$_2$	{d[T$_B$T$_A$(GC)$_3$]}$_2$
	(a) {d(GC)$_3$}$_2$ Family		
T_BH6			*a*
T_B(CH_3)			25.5
T_AH6			*a*
T_A(CH_3)			73.0
C_2H5	65.0	60.5	*b*
C_2H6	59.5	62.0	65.0
C_4H5	59.0	63.5	*b*
C_4H6	69.0	66.0	73.5
C_6H5	50.5	*b*	*b*
C_6H6	57.0	67.5	67.0
T_AH6		55.0	
T_A(CH_3)			
T_BH6		46.5	
T_B(CH_3)		45.0	
av t_m[c]	60.0	63.9	68.5
global t_m[d]	66.0	71.2	72.4
	(b) {d(CG)$_3$}$_2$ Family		
proton	{d(C$_1$GC$_3$GC$_5$G)}$_2$	{d[(CG)$_3$T$_A$T$_B$]}$_2$	{d[T$_B$T$_A$(CG)$_3$]}$_2$
T_BH6			*a*
T_B(CH_3)			63.0
T_AH6			66.0
T_A(CH_3)			63.0
C_1H5	57.5	65.6	66.0
C_1H6	*a*	48.0	57.0
C_3H5	57.5	76.0	70.0
C_3H6	59.5	67.5	77.7
C_5H5	45.0	73.0	69.5
T_AH6		*a*	
T_A(CH_3)		43.0	
T_BH6		*a*	
T_B(CH_3)		*a*	
av t_m[c]	56.2	65.3	68.8
global t_m[d]	68.7	67.0	71.9

[a] Chemical shift versus temperature profile did not permit a t_m to be defined. [b] Not assigned due to spectral overlap. [c] Average t_m was calculated by taking an average of the CH5 and CH6 values and does not include the thymidine TH6 and CH_3 t_m's. [d] Global t_m was extrapolated to the NMR concentrations by using eq 1.

Computer Modeling. To help rationalize the greater thermal stabilization induced by 5′ versus 3′ dangling thymidine residues, we have used computer graphics to model the structural features of each duplex. The resulting computer-generated structures are shown in Figure 5. In this modeling, we have assumed that each DNA duplex structure adopts a B conformation and we have used Arnott coordinates. This assumption is consistent with our CD spectra. We further assumed that the unpaired thymidine residues adopt positions in space that allow them to extend the B conformation beyond the core duplex. This last assumption leads to the intriguing observation that the 5′ dangling thymidine residues assume conformations that allow them to more effectively stack on the core duplex compared with the 3′ dangling thymidine residues. This positional dependence for the stacking of dangling residues may help provide a structural explanation for the optical and NMR results we have reported here. Similar computer modeling studies on RNA duplexes with dangling residues have been conducted by Freier et al. (1986a–c). Their computer modeling reveals that for RNA duplexes in the A conformation the 3′ dangling residues stacked more efficiently on the core duplex than the corresponding 5′ dangling residues. Significantly, Freier et al. found that in RNA duplexes 3′ dangling residues increase the melting temperatures more than 5′ dangling residues. Thus, computer modeling successfully rationalizes the opposite positional influences of dangling ends on the thermal stabilities of RNA and DNA duplex structures.

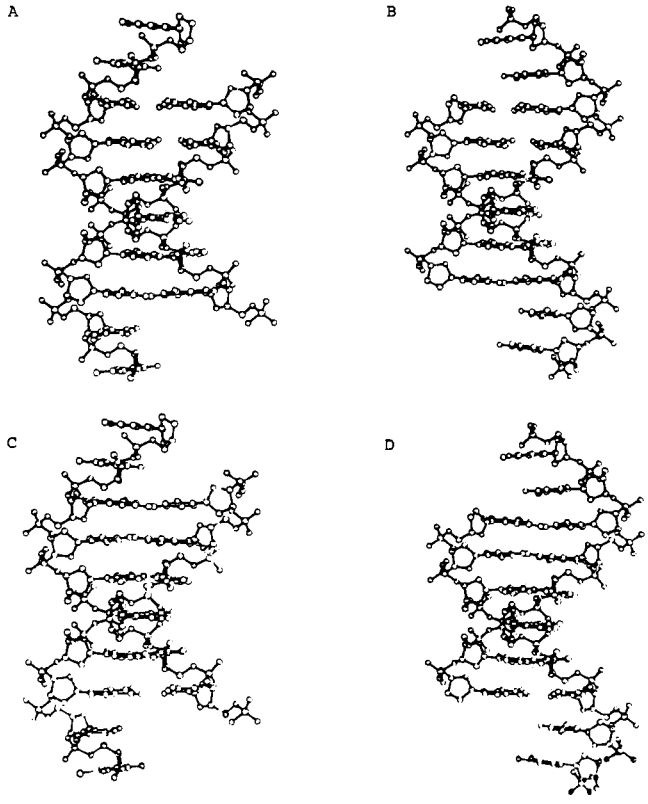

FIGURE 5: Computer-generated molecular models of the dangling end molecules in the B-helical conformation using Arnott coordinates: (a) $\{d[(GC)_3TT]\}_2$, (b) $\{d[TT(GC)_3]\}_2$, (c) $\{d[(CG)_3TT]\}_2$, and (d) $\{d[TT(CG)_3]\}_2$.

ACKNOWLEDGMENTS

We thank Professor Wilma Olson and Dr. A. R. Srinivasan for their assistance and advice with the computer modeling studies.

SUPPLEMENTARY MATERIAL AVAILABLE

Two figures showing HPLC chromatograms of duplexes I–VI after final purification and after enzymatic degradation and one figure showing CD spectra of duplexes containing dangling thymidines (3 pages). Ordering information is given on any current masthead page.

REFERENCES

Albergo, D. D., Marky, L. A., Breslauer, K. J., & Turner, D. H. (1981) *Biochemistry 20*, 1409–1413.

Ayer, D., & Yarus, M. (1986) *Science (Washington, D.C.) 231*, 393–395.

Breslauer, K. J. (1986) in *Thermodynamic Data for Biochemistry and Biotechnology* (Hinz, H., Ed.) pp 402–427, Springer-Verlag, Seacaucus, NJ.

Breslauer, K. J., Sturtevant, J. M., & Tinoco, I., Jr. (1975) *J. Mol. Biol. 99*, 549–565.

Breslauer, K. J., Frank, R., Blocker, H., & Marky, L. A. (1986) *Proc. Natl. Acad. Sci. U.S.A. 83*, 3746–3750.

Cantor, C., Warshaw, M. W., & Shapiro, H. (1970) *Biopolymers 9*, 1059–1077.

Cheng, D. M., Kan, L. S., Frechet, D., Ts'o, P. O. P., Uesugi, S., Shida, T., & Ikehara, M. (1984) *Biopolymers 23*, 775–795.

Freier, S. M., Alkema, D., Sinclair, A., Neilson, T., & Turner, D. H. (1985) *Biochemistry 24*, 4533–4539.

Freier, S. M., Sugimoto, N., Sinclair, A., Alkema, D., Neilson, T., Kierzek, R., Caruthers, M. H., & Turner, D. H. (1986a) *Biochemistry 25*, 3214–3219.

Freier, S. M., Kierzek, R., Caruthers, M. H., Neilson, T., & Turner, D. H. (1986b) *Biochemistry 25*, 3209–3213.

Freier, S. M., Kierzek, R., Jaeger, J. A., Sugimoto, N., Caruthers, M. H., Neilson, T., & Turner, D.H. (1986c) *Proc. Natl. Acad. Sci. U.S.A. 83*, 9373–9377.

Gaffney, B. L., Marky, L. A., & Jones, R. A. (1984) *Biochemistry 23*, 5686–5691.

Grosjean, H., Soll, D. G., & Crothers, D. M. (1976) *J. Mol. Biol. 103*, 499–519.

Kim, S. H., Suddath, F. L., Quigley, G. J., McPherson, A., Sussman, J. L., Wang, A. H. J., Seeman, N. C., & Rich, A. (1974) *Science (Washington, D.C.) 185*, 435–440.

Marky, L. A., & Breslauer, K. J. (1987) *Biopolymers 26*, 1601–1620.

Marky, L. A., Jones, R. A., & Breslauer, K. J. (1982) *Biophys. J. 37*, 3060a.

Martin, F. H., Uhlenbeck, O. C., & Doty, P. (1971) *J. Mol. Biol. 57*, 201–215.

Mellema, J., van der Woerd, R., van der Marel, G. A., van Boom, J. H., & Altona, C. (1984) *Nucleic Acids Res. 12*, 5061–5078.

Petersheim, M., & Turner, D. H. (1983) *Biochemistry 22*, 256–263.

Richards, E. G. (1975) *Handb. Biochem. Mol. Biol., 3rd Ed.* 1, 197.

Robertus, J. D., Ladner, J. E., Finch, J. T., Rhodes, D., Brown, R. D., Clark, B. F. C., & Klug, A. (1974) *Nature (London) 250*, 546–551.

Romaniuk, P. J., Hughes, D. W., Gregoire, R. J., Neilson, T., & Bell, R. A. (1978) *J. Am. Chem. Soc. 100*, 3971–3972.

Senior, M. M., Jones, R. A., & Breslauer, K. J. (1985) *Biophys. J. 47*, 226a.

Sugimoto, N., Kierzek, R., & Turner, D. H. (1987) *Biochemistry 26*, 4554–4558.

Turner, D. H., Sugimoto, N., Kierzek, R., & Dreiker, S. D. (1987) *J. Am. Chem. Soc. 109*, 3783–3785.

Yoon, K., Turner, D. H., Tinoco, I., Jr., von der Haar, F., & Cramer, F. (1976) *Nucleic Acids Res. 3*, 2233–2241.